

Quantum Instability

Michael Q. May* and Hong Qin†

Plasma Physics Laboratory, Princeton University, Princeton, NJ 08540, U.S.A

Abstract

The physics of many closed, conservative systems can be described by both classical and quantum theories. The dynamics according to classical theory is symplectic and admits linear instabilities which would initially seem at odds with a unitary quantum description. Using the example of three-wave interactions, we describe how a time-independent, finite-dimensional quantum system, which is Hermitian with all real eigenvalues, can give rise to a linear instability corresponding to that in the classical system. We show that the instability is realized in the quantum theory as a cascade of the wave function in the space of occupation number states, and an unstable quantum system has a richer spectrum and a much longer recurrence time than a stable quantum system. The conditions for quantum instability are described.

arXiv:2208.03371v1 [quant-ph] 5 Aug 2022

* mqmay@princeton.edu

† hongqin@princeton.edu

I. INTRODUCTION

Many physical processes, in particular the dynamics of closed conservative systems, may be usefully described by both quantum and classical theories. However, classical dynamics are governed by Hamilton's equations whose solutions are symplectic maps, while quantum dynamics, governed by the Schrödinger equation, are unitary. A consequential difference between symplectic maps and unitary maps is that the former allow for dynamical instabilities and the latter do not. Traditionally, this has required investigations into instabilities to occur solely within the classical domain. For example, an opto-mechanical system, where light in a resonant cavity is coupled to a mechanical arm which affects the size of the cavity, can be described quantum mechanically in terms of photons and phonons. But recent work dealing with the opto-mechanical instability used a semi-classical approach rather than the quantum description [1–3]. This motivates the question of how to describe dynamical instabilities using quantum mechanics. The issue of instabilities in quantum mechanics has received some attention in the past, particularly concerning transitions to chaotic behavior [4], time-dependent Hamiltonians [5], PT-symmetric Hamiltonians [6–12], and pseudo-Hermitian Hamiltonians [13]. Despite these studies, the fundamental question of how to characterize a quantum instability in a time-independent, finite Hermitian Hamiltonian has been unaddressed. In classical dynamical systems, a linear instability is characterized by the existence of an eigenfrequency with positive imaginary part, i.e, growth rate. This is impossible in a closed quantum system since the dynamics are unitary, and its eigenfrequencies are real. However, the unitary nature of Hermitian quantum systems does not preclude the exponential growth of an observable that does not commute with the Hamiltonian. In the present study, we define the concept of a quantum instability as follows.

Definition 1. For a linear Hermitian quantum system with time-independent parameters, an instability of an observable is a solution of the system for which the expected value of the observable deviates exponentially from the initial condition. When such an instability exists, the quantum system is said to be unstable with respect to the observable.

In this paper, we will use the three-wave interaction model to illustrate how a such quantum instability occurs. Characterizing such quantum instabilities is not only of academic interest, but also has practical value for identifying when they can be realized or inevitably occur on quantum systems. The three-wave interaction, which experiences a

classical instability, was recently simulated on a quantum computer [14]. Although the simulation was not of high enough dimension to allow for the instability, it demonstrates the importance of the present work.

The three-wave interaction, the lowest order nonlinear interaction in plasma dynamics, has applications in laser-plasma interactions [15, 16], determining weak turbulence spectra [17], and nonlinear optical system design [18–20]. Classically, the linear dynamics of the interaction are affected by a parametric instability before developing into the nonlinear regime [21]. Physically, this instability is triggered when one large amplitude wave denoted by (ω_1, k_1) resonate with two others, denoted by (ω_2, k_2) and (ω_3, k_3) . In the so-called decay interaction the resonance conditions are $\omega_1 = \omega_2 + \omega_3$ and $k_1 = k_2 + k_3$, which ensure energy-momentum conservation. The instability transfers energy-momentum from the large wave to the two smaller waves. Although this interaction and instability are well-known [22–25], its quantum description is less studied [14, 21, 26–28], and the correspondence between the classical instability and its quantum counterpart has not been established.

Section II will focus on providing background to the classical three-wave instability and the quantum theory of three-wave interaction by Shi *et al.* [14, 21, 27, 28]. In Sec. III, the quantum three-wave interaction equation will be approximately solved in the linear regime, and an unstable solution will be found, demonstrating the existence of a quantum instability according to Definition 1. This unstable quantum solution will be compared with the classical solution, and the classical limit of the quantum instability will be discussed. Numerical results showing the validity of the approximate linear solution of the quantum instability will also be presented. In Sec. IV, we will show how the quantum instability is realized as a cascade of the wave function in the space of the occupation number states. The expected occupation number of a quantum solution in terms of the eigenvalues of the Hamiltonian will be derived. It shows a richer spectrum in the unstable system than in the stable system. The eigenvalues of the stable Hamiltonian are linearly distributed, while the eigenvalues of the unstable Hamiltonian are nonlinearly distributed. Finally, Sec. V concludes with a discussion of the requirements for realizing the quantum instability on quantum hardware and of future work to be done on quantum instabilities.

II. THE THREE-WAVE INTERACTION

In an ordinary gas, sound waves may nonlinearly self-steepen due to interactions between the principle wave and its higher frequency resonances. This is possible because each of the wave frequencies is a normal mode of the system and therefore allowed. By contrast, most plasmas' dispersion relations are very dispersive, so nonlinear interactions of a single wave with its higher frequency resonances are negligible. The lowest order nonlinear interaction in plasma dynamics is thus the three-wave interaction, where a single wave interacts resonantly with two others. For example, two Alfvén waves can interact nonlinearly with a sound wave in a homogeneous plasma [29].

A. Classical theory for three-wave interaction and instability

In the classical theory, the nonlinear dynamics of the homogeneous three-wave interaction may be reduced to [24, 25, 30, 31]

$$\partial_t A_1 = g A_2 A_3, \quad (1)$$

$$\partial_t A_2 = -g^* A_1 A_3^*, \quad (2)$$

$$\partial_t A_3 = -g^* A_1 A_2^*, \quad (3)$$

where g is a coupling coefficient, A_j is the amplitude of the j -th wave, and A_j^* its complex conjugate. Equations (1)-(3) are the canonical Hamilton's equations corresponding to the Hamiltonian

$$H = g A_1^* A_2 A_3 - g^* A_1 A_2^* A_3^*, \quad (4)$$

for the canonical pairs of A_j and A_j^* . By choosing an appropriate normalization, we can let $g = 1$ without losing generality. The governing equations for the wave action $I_j = |A_j|^2$ are found to be

$$\partial_t I_1 = -\partial_t I_2 = -\partial_t I_3 = g A_1^* A_2 A_3 + g^* A_1 A_2^* A_3^*. \quad (5)$$

These obviate two constants of motion in the system,

$$s_2 = I_1 + I_3, \quad (6)$$

$$s_3 = I_1 + I_2, \quad (7)$$

so that the growth of the second or third waves will reduce the amplitude of the first. Using these constants of motion while taking another time derivative of Eq. (5), we arrive at closed equations for the classical wave actions,

$$\partial_t^2 I_1 = 2 \left(s_2 s_3 + 3I_1^2 - 2(s_2 + s_3) I_1 \right), \quad (8)$$

$$\partial_t^2 I_2 = 2 \left(s_3(s_2 - s_3) - 3I_2^2 + 2(2s_3 - s_2) I_2 \right), \quad (9)$$

$$\partial_t^2 I_3 = 2 \left(s_2(s_3 - s_2) - 3I_3^2 + 2(2s_2 - s_3) I_3 \right). \quad (10)$$

Note that Eq. (5) implies that the right hand sides of Eqs. (8)-(10) are equivalent up to a sign change. Equations (8)-(10) are second-order nonlinear differential equations which may be solved in terms of elliptic integrals, and in the special case that $I_2 = I_3$ the solutions for I_1 , I_2 , and I_3 take on particularly simple forms in terms of hyperbolic tangent and secant, respectively.

The linear instability of the three-wave system can be equivalently described using Eqs. (1)-(3) or Eqs. (8)-(10). For easy comparison with the quantum result in the next section, we analyze the classical three-wave instability using Eqs. (8)-(10).

In classical theory, linear instability refers to the exponential growth of a deviation relative to an equilibrium solution of a system. For the system studied here, the equilibrium solution of Eqs. (8)-(10) is $I_{10} = \text{const.} \neq 0$ and $I_{20} = I_{30} = 0$. Consider a perturbation of the system of the form,

$$I_1 = I_{10} + \delta I_1, \quad (11)$$

$$I_2 = \delta I_2, \quad (12)$$

$$I_3 = \delta I_3. \quad (13)$$

The linearized system for δI_1 , δI_2 , and δI_3 is

$$\partial_t^2 \delta I_1 = 0, \quad (14)$$

$$\partial_t^2 \delta I_2 = 4I_{10} \delta I_2, \quad (15)$$

$$\partial_t^2 \delta I_3 = 4I_{10} \delta I_3. \quad (16)$$

Thus, the system is unstable with growth rate $\gamma = 2\sqrt{I_{10}}$. However, only δI_2 and δI_3 grow exponentially with time. Equations (1) and (14) indicate that for the unstable eigenmode of the linearized system, δI_1 and δA_1 remain constant.

As will be shown in Sec. III, an equilibrium solution for the quantum system cannot be meaningfully defined. Therefore, for comparison with the quantum solution, we derive the linear dynamics of Eqs. (8)-(10) relative to an initial condition $I_j(0) = I_{ji} \neq 0$ ($j = 1, 2, 3$). For exact solutions, s_2 and s_3 are conserved, so a solution for I_1 will determine the solutions for I_2 and I_3 . Assuming an initial condition and a small deviation of the form

$$I_j = I_{ji} + \delta I_j, \quad (j = 1, 2, 3), \quad (17)$$

Eq. (8) can be rewritten as

$$\partial_t^2 \delta I_1 = 2(\delta I_1(2(I_{1i} - I_{2i} - I_{3i}) + 3\delta I_1) + I_{2i}I_{3i} - I_{1i}(I_{2i} + I_{3i})). \quad (18)$$

Assuming that $\delta I_1 \ll \frac{2}{3}(I_{1i} - I_{2i} - I_{3i})$, which will be true for short times, we may ignore the term proportional to δI_1^2 ,

$$\partial_t^2 \delta I_1 = 2(\delta I_1 2(I_{1i} - I_{2i} - I_{3i}) + I_{2i}I_{3i} - I_{1i}(I_{2i} + I_{3i})). \quad (19)$$

Its solution is

$$\delta I_1 = \frac{B_C}{\gamma_C^2} + C_1 e^{\gamma_C t} - \left(\frac{B_C}{\gamma_C^2} + C_1 \right) e^{-\gamma_C t}, \quad (20)$$

where,

$$\gamma_C = 2\sqrt{I_{1i} - I_{2i} - I_{3i}}, \quad (21)$$

$$B_C = 2I_{1i}(I_{2i} + I_{3i}) - 2I_{2i}I_{3i}. \quad (22)$$

The classical constants γ_C and B_C are written with a subscript ‘‘C’’ to distinguish them from quantum constants γ_Q and B_Q which will be derived in the next section. The third constant C_1 cannot be determined from the action equations, Eq. (19) and its counterparts for I_2 and I_3 , because they each only involve even time derivatives at the zeroth and second order. To determine C_1 , the first order Eqs. (1)-(3) must be used. Choosing $(A_1(0), A_2(0), A_3(0)) = (\sqrt{I_{1i}}, \sqrt{I_{2i}}, \sqrt{I_{3i}})$, we find

$$C_1 = \frac{\sqrt{I_{1i}I_{2i}I_{3i}}}{\gamma_C} - \frac{B_C}{\gamma_C^2}. \quad (23)$$

The growth rate γ_C recovers the growth rate γ derived above when $I_{2i} = I_{3i} = I_{20} = I_{30} = 0$.

B. Quantum theory for three-wave interaction

The quantum theory for three-wave interaction is formulated by the field-theoretical method, i.e. by quantizing the classical fields A_j as quantum operators \hat{A}_j on the occupation number states. The resulting Hamiltonian for a homogeneous (spatially independent) quantum three-wave interaction with complex coupling constant g is [14, 21, 27, 28]

$$\hat{H} = ig\hat{A}_1^\dagger\hat{A}_2\hat{A}_3 - ig^*\hat{A}_1\hat{A}_2^\dagger\hat{A}_3^\dagger, \quad (24)$$

where the \hat{A}_j^\dagger , \hat{A}_j ($j = 1, 2, 3$) are creation and annihilation operators, respectively, and $[\hat{A}_j, \hat{A}_l^\dagger] = \delta_{jl}$. This Hamiltonian acts on the space of occupation number states $|n_1, n_2, n_3\rangle$, and commutes with operators $\hat{s}_2 = \hat{n}_1 + \hat{n}_3$ and $\hat{s}_3 = \hat{n}_1 + \hat{n}_2$, where the $\hat{n}_j = \hat{A}_j^\dagger\hat{A}_j$ are standard number operators. The \hat{s}_2 and \hat{s}_3 operators are identical in form to the constants of motion found in the classical theory, Eqs. (6) and (7), so we will write their expectation values identically, i.e. $\langle\hat{s}_2\rangle = s_2$ and $\langle\hat{s}_3\rangle = s_3$.

Because \hat{s}_2 and \hat{s}_3 commute with \hat{H} , their eigenstates form an invariant subspace of dimension $d = s_2 + 1$ [14, 28] with states

$$\Psi(t) = \sum_{i=0}^{s_2} \alpha_i(t)\psi_i, \quad (25)$$

where,

$$\psi_i = |s_2 - i, s_3 - s_2 + i, i\rangle. \quad (26)$$

It is assumed that the eigenvalue $s_3 \geq s_2$, which accounts for the asymmetry in the above equation. Within this subspace, the Hamiltonian is represented as a square tridiagonal matrix with vanishing diagonal. Taking the coupling constant $g = -i$, the matrix is also symmetric, with elements

$$H_{ij} = \delta_{i,j+1}h_i + \delta_{i+1,j}h_j, \quad (27)$$

$$h_i = \sqrt{(s_2 - i)(s_3 - s_2 + 1 + i)(i + 1)}. \quad (28)$$

As will be shown below, the phase of the coupling constant will not affect the dynamics of observables. Also, we emphasize that this quantization procedure using the field-theoretical method maps the classical nonlinear Hamiltonian specified by Eq. (4) into a quantum (linear) Hamiltonian operator on a finite-dimensional Hilbert space.

Recently, the quantum three-wave interaction was simulated by Shi *et al.* [14] on a Rigetti Computing hardware using a system with $d = 3$. By realizing the unitary operator as a single gate, they were able to robustly simulate the quantum three-wave interaction an order of magnitude longer than by approximating the unitary operator as a series of native gates.

Returning to Eq. (24) with an arbitrary coupling coefficient g , the Heisenberg equations are

$$\begin{aligned}\partial_t \hat{A}_1 &= g \hat{A}_2 \hat{A}_3, \\ \partial_t \hat{A}_2 &= -g^* \hat{A}_1 \hat{A}_3^\dagger, \\ \partial_t \hat{A}_3 &= -g^* \hat{A}_1 \hat{A}_2^\dagger,\end{aligned}\tag{29}$$

which are identical in form to the amplitude equations of the classical case, Eqs. (1)-(3), with classical wave amplitudes replaced by operators. Also as with the classical case, we may combine these equations using the constants of motion to find decoupled second-order equations for the number operators $\hat{n}_j = \hat{A}_j^\dagger \hat{A}_j$,

$$\partial_\tau^2 \hat{n}_1 = 2 \left(\hat{s}_2 \hat{s}_3 + 3 \hat{n}_1^2 - (2 \hat{s}_2 + 2 \hat{s}_3 + 1) \hat{n}_1 \right),\tag{30}$$

$$\partial_\tau^2 \hat{n}_2 = 2 \left(\hat{s}_3 (1 + \hat{s}_2 - \hat{s}_3) - 3 \hat{n}_2^2 + (4 \hat{s}_3 - 2 \hat{s}_2 - 1) \hat{n}_2 \right),\tag{31}$$

$$\partial_\tau^2 \hat{n}_3 = 2 \left(\hat{s}_2 (1 + \hat{s}_3 - \hat{s}_2) - 3 \hat{n}_3^2 + (4 \hat{s}_2 - 2 \hat{s}_3 - 1) \hat{n}_3 \right),\tag{32}$$

where $\tau = t|g|$, and $\partial_\tau^2 \hat{n}_1 = -\partial_\tau^2 \hat{n}_2 = -\partial_\tau^2 \hat{n}_3$. Note that Eqs. (30)-(32) depend only on the magnitude of the coupling constant, which has been absorbed by the normalized time parameter. Next, to fairly compare the quantum and classical equations, we take the expectation of Eqs. (30)-(32),

$$\partial_\tau^2 \langle n_1 \rangle = 2 \left(s_2 s_3 + 3 \langle n_1^2 \rangle - (2s_2 + 2s_3 + 1) \langle n_1 \rangle \right),\tag{33}$$

$$\partial_\tau^2 \langle n_2 \rangle = 2 \left(s_3 (1 + s_2 - s_3) - 3 \langle n_2^2 \rangle + (4s_3 - 2s_2 - 1) \langle n_2 \rangle \right),\tag{34}$$

$$\partial_\tau^2 \langle n_3 \rangle = 2 \left(s_2 (1 + s_3 - s_2) - 3 \langle n_3^2 \rangle + (4s_2 - 2s_3 - 1) \langle n_3 \rangle \right).\tag{35}$$

Directly comparing the classical Eqs. (8)-(10) with their quantum counterparts defined above, we see that as with the classical case, the right hand sides of Eqs. (30), (31), and (32) differ only by their signs. There are also significant differences. Each equation now includes additional factors of the number of photons $\langle n_j \rangle$ on the right hand side of the equations, and

the last two equations also include additional constant factors. More importantly, the quantum and classical second-order equations differ in that the quantum equations are not closed equations for photon number $\langle n_j \rangle$. They also depend on the variance $\delta_j = \langle n_j^2 \rangle - \langle n_j \rangle^2$. As will be discussed in Sec. III, the variance cannot be zero for all times except in the trivial solution $\langle n_1 \rangle = \langle n_2 \rangle = \langle n_3 \rangle = 0$. Since the variance is nonzero, either a closure must be established for Eqs. (33)-(35) to be useful, or the full Schrödinger equation must be solved numerically.

III. THE QUANTUM THEORY OF THREE-WAVE INSTABILITY

In this section, we find an approximate solution for $\langle n_1 \rangle(\tau)$ which corresponds to the exponential growth of the unstable classical solution as discussed in Sec. II. This first requires assuming an initial condition so as to determine the variance δ_j . With an expansion of the variance, we then linearize Eq. (33) and find the growth rate of the quantum instability. The unstable solutions according to the classical and quantum descriptions of the three-wave interaction are compared. Finally, the approximate solution is validated by the numerical solution of the Schrödinger equation.

A. Approximate solution of the variance

We seek to solve Eq. (33), which depends on the variance δ_1 . Estimating δ_1 requires considering the Schrödinger equation

$$i\partial_\tau \Psi = H\Psi, \tag{36}$$

where the Hamiltonian H is defined in Eq. (24) and the constant $\hbar = 1$. The Hamiltonian for the invariant subspace of constant s_2 and s_3 is a $d \times d$ matrix,

$$H = \begin{pmatrix} 0 & h_0 & 0 & 0 & 0 & \dots \\ h_0 & 0 & h_1 & 0 & 0 & \dots \\ 0 & h_1 & 0 & h_2 & 0 & \dots \\ 0 & 0 & h_2 & 0 & h_3 & \dots \\ \vdots & \vdots & \vdots & \vdots & \vdots & \ddots \end{pmatrix}, \tag{37}$$

where h_j are defined by Eq. (24). Equation (36) is a system of d coupled first-order differential equations,

$$i\dot{\alpha}_0 = h_0\alpha_1, \quad (38)$$

$$i\dot{\alpha}_1 = h_0\alpha_0 + h_1\alpha_2, \quad (39)$$

...

$$i\dot{\alpha}_i = h_{i-1}\alpha_{i-1} + h_i\alpha_{i+1}. \quad (40)$$

which are written explicitly in terms of the basis vectors ψ_i defined in Eqs. (25) and (26). As basis vectors in this d dimensional space, ψ_i can be represented as

$$\psi_i = (\underbrace{0, 0, \dots, 0}_i, 1, 0, 0, \dots, 0). \quad (41)$$

As a footnote, we point out that it is straightforward to show by construction that there exists a unique nontrivial equilibrium solution such that $\dot{\alpha}_i = 0$ for all i . However, this zero-energy eigenstate should not be viewed as the quantum counterpart of the equilibrium in the classical theory.

The variance of the observable \hat{n}_1 is

$$\begin{aligned} \delta &= \langle n_1^2 \rangle - \langle n_1 \rangle^2 \\ &= \sum_{j=0}^{s_2} |\alpha_j|^2 (s_2 - j)^2 - \left(\sum_{j=0}^{s_2} |\alpha_j|^2 (s_2 - j) \right)^2. \end{aligned} \quad (42)$$

Note that for an infinitely narrow initial condition, where $\alpha_m(0) = 1$ and $\alpha_{i \neq m}(0) = 0$ for some m , the variance is zero. Using the above expression of δ_1 , it can also be proven that its maximum value is $s_2^2/4$.

For a sufficiently narrow distribution of initial states, it may be possible to approximate the variance as a constant, so long as it does not grow too quickly in time. To justify this approximation, consider a narrowly distributed initial condition

$$\Psi(0) = (\alpha_0(0), \alpha_1(0), \dots, \alpha_{s_2}(0)) = (\dots, \phi\varepsilon^2, \phi\varepsilon, \phi, \phi\varepsilon, \phi\varepsilon^2, \dots), \quad (43)$$

where ϕ is a normalization such that $\sum_{i=0}^{s_2} |\alpha_i(0)|^2 = 1$, and $\varepsilon \ll 1$ is a small parameter describing how spread out the initial state is. Algebraically, this requires that for

some m , $\alpha_i(0) = \varepsilon^{|m-i|}\alpha_m(0)$, i.e., the initial distribution is centered around the m -th state $|n_1, n_2, n_3\rangle = |s_2 - m, s_3 - s_2 + m, m\rangle$. At $\tau = 0$, the variance of \hat{n}_1 according to Eq. (42) is

$$\delta_1(\tau = 0) = \frac{2\varepsilon^2(1 - \varepsilon^2)}{(1 + \varepsilon^2)^2} \sum_{n=0}^{\infty} \varepsilon^{2n}(2n(n+1) + 1). \quad (44)$$

Then, assuming the time τ and spreading parameter ε are small, we may expand Eqs. (38)-(40) in terms of these small parameters to find the variance δ_1 as a series in orders of ε and τ . To first order in τ , δ_1 is also first order in ε ,

$$\delta_1(\tau) = \delta_1(\tau = 0) + 2\varepsilon\tau(h_m - h_{m-1}) + \mathcal{O}(\tau^2) + \mathcal{O}(\varepsilon^2). \quad (45)$$

Note that it happens that each order in τ introduces a factor of a constant $h_i \sim h_m$, so we require that $\tau \ll 1/h_m$ for the expansion to hold. Thus, the growth of the variance δ_1 is linearly proportional to the small spreading parameter ε at short times, and we may provisionally take $\delta_1(\tau) = \delta_1(0)$, relying on the smallness of ε . We will check this assumption numerically below.

B. Quantum three-wave instability

We now proceed to solve Eq. (33) for a narrowly distributed initial condition described in Eq. (43). Denote by $(\langle n_1 \rangle, \langle n_2 \rangle, \langle n_3 \rangle) = (n_{1i}, n_{2i}, n_{3i})$, the initial expected occupation numbers. Letting $\langle n_1 \rangle = n_{1i} + \delta n_1$, and Taylor expanding Eq. (33) around n_{1i} , we have

$$\delta \ddot{n}_1 = 2(3\delta_1(\tau) + n_{2i}n_{3i} - n_{1i}(1 + n_{2i} + n_{3i}) + \delta n_1(2n_{1i} - 2n_{2i} - 2n_{3i} - 1 + 3\delta n_1)). \quad (46)$$

Collecting terms allows us to define

$$\gamma_Q = 2\sqrt{n_{1i} - n_{2i} - n_{3i} - 1/2}, \quad (47)$$

and

$$B_Q(\tau) = 2n_{1i}(1 + n_{2i} + n_{3i}) - 2n_{2i}n_{3i} - 6\delta_1(\tau), \quad (48)$$

similarly to the classical definitions of γ_C and B_C , Eqs. (21) and (22). Thus, Eq. (46) can be written as

$$\delta \ddot{n}_1 = \delta n_1(\gamma_Q^2 + 6\delta n_1) - B_Q(\tau). \quad (49)$$

As in the classical case, when $\tau \ll 1/\gamma_Q$ (or equivalently $\delta n_1 \ll \gamma_Q^2$), the quadratic term may be neglected. Since the growth of δ_1 may be made arbitrarily small with ϵ , let us assume a constant variance such that $B_Q(\tau) = B_Q(0) \equiv B_Q$. This results in an approximate quantum three-wave interaction equation,

$$\delta \ddot{n}_1 = \delta n_1 \gamma_Q^2 - B_Q, \quad (50)$$

which is identical in form to the classical equation, Eq. (19), and also shares a solution of the same form

$$\delta n_1 = \frac{B_Q}{\gamma_Q^2} + C_1 e^{\gamma_Q \tau} + \left(\frac{B_Q}{\gamma_Q^2} + C_1 \right) e^{-\gamma_Q \tau}, \quad (51)$$

where C_1 is a constant determined by the initial conditions. The above equation for δn_1 implies that the condition for instability in the quantum theory of the three-wave interaction (assuming an initial variance which grows slowly in time) is similar to the classical instability criterion, namely that $\gamma_Q^2 > 0$.

Since it is not possible to formulate a first-order equation for $\langle n_1 \rangle$ in lieu of the second-order Eqs. (30)-(32), the constant C_1 must be calculated directly from the Schrödinger equation at $\tau = 0$. Explicitly,

$$\delta \dot{n}_1(0) = \partial_\tau \langle n_1 \rangle(0) = \sum_{i=0}^{s_2} 2\alpha_i(0) \dot{\alpha}_i(0) (s_2 - i), \quad (52)$$

where the time-derivatives of the weights α_i are given by Eqs. (38)-(40).

C. Classical Correspondence

In summary, we have found that the quantum theory for three-wave interaction supports a quantum instability according to Definition 1. This quantum instability corresponds to the classical description of the instability, and the unstable solutions are structurally identical. Both require that the growth rate γ is real for an instability, and both are only applicable so long as the quadratic terms δI_1^2 and δn_1^2 are small. The growth rates,

$$\begin{aligned} \gamma_Q &= 2\sqrt{n_{1i} - n_{2i} - n_{3i} - 1/2}, \\ \gamma_C &= 2\sqrt{I_{1i} - I_{2i} - I_{3i}}, \end{aligned}$$

and other constants of the unstable solutions,

$$B_Q = 2n_{1i}(1 + n_{2i} + n_{3i}) - 2n_{2i}n_{3i} - 6\delta_1(0),$$

$$B_C = 2I_{1i}(I_{2i} + I_{3i}) - 2I_{2i}I_{3i},$$

differ only by constant factors, and the relative differences between these constants tend towards zero in the classical limit as $n_{1i}, n_{2i}, n_{3i} \rightarrow \infty$. Further, for a fixed spreading parameter $\varepsilon < 1$, the initial condition described in Eq. (43) will yield a variance that approaches zero in the classical limit.

There are crucial differences between the quantum and classical systems which do not diminish as the photon number increases though. First, the quantum wave action equation, Eq. (33), depends on the variance of the action, a purely quantum phenomenon. Although the effect of the variance on the approximate quantum solution may be reduced if the initial variance is chosen to be small, it still introduces a new independent parameter which must be chosen carefully to result in instability. Second, the quantum system does not admit closed first-order equations for the wave amplitude as the classical system does in Eq. (5). This has the effect of making the constant C_1 in Eq. (51) non-trivial to calculate in the quantum system, and since C_1 depends on the initial variance, it will not in general converge to the classical value in the classical limit. Finally, the quantum theory does not have a zero-energy eigenstate corresponding to the classical equilibrium. The classical and quantum solutions being compared are the result of linearizations about an arbitrary initial condition instead of an equilibrium.

D. Numerical solution of quantum instability

In this subsection, we compare the approximate solution of quantum instability obtained with the numerical solution of the Schrödinger equation. For a fixed s_2 and s_3 , we expect the quantum instability to have the highest growth rate when $(\langle n_1 \rangle(0), \langle n_2 \rangle(0), \langle n_3 \rangle(0) \equiv (n_{1i}, n_{2i}, n_{3i}) = (s_2, 0, 0)$ and $s_2 = s_3$. This follows from the definition of the growth rate of the instability γ_Q in Eq. (47). Indeed, in the next section, this case will be used as the example of quantum instability. For evaluating the validity of the approximate solution of quantum instability, Eq. (51), this system is the most favorable because its initial variance δ_1 and spreading parameter ε are zero.

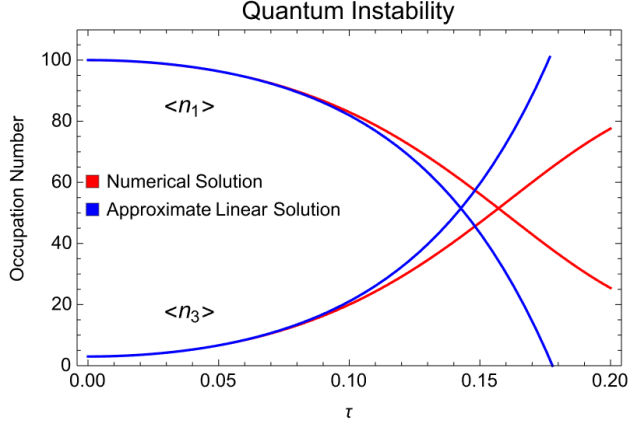


Figure 1: Numerical solution of the Schrödinger equation, Eq. (36), and approximate linear solution, Eq. (51), of quantum system with the unstable initial condition $(n_{1i}, n_{2i}, n_{3i}) = (100, 10, 3)$. The spreading parameter is $\varepsilon = 0.1$, which yields $\delta_1(0) = 0.02$ and $C_1 = -3.9$.

Here, we consider a less favorable unstable initial condition $(n_{1i}, n_{2i}, n_{3i}, \varepsilon) = (100, 10, 3, 0.1)$. Plotted in Fig. 1 are the exact quantum solution to the Schrödinger equation and the approximate solution of Eq. (51) for that initial condition. Note that while the derivation of the solution to the linearized Eq. (50) is only valid until $\tau \sim 1/h_{z_0} = 0.02$ as required by our expansion of the variance in Eq. (45), the linearized solution matches the exact solution well beyond that point. At $\tau \sim 0.14$, the condition for the linearization, $\delta n_1 \ll \gamma_Q^2$, breaks as $\delta n_1 \cong 50$ and $\gamma_Q^2 = 346$, and the approximate solution and exact solutions diverge. In the case of $(n_{1i}, n_{2i}, n_{i0}, \varepsilon) = (100, 0, 0, 0)$, the approximate solution remains valid much longer since the growth of the variance δ_1 is now second order in τ as shown in Eq. (45), and the initial condition imposes $\langle \dot{n}_1 \rangle(0) = 0$, keeping δn_1 smaller than γ_Q^2 for much longer.

IV. PROPERTIES OF QUANTUM INSTABILITY

In this section, we investigate the properties of the quantum instability through numerical solutions. It is demonstrated that the quantum instability is realized as a cascade of wave functions in the space of occupation number states. We also show that an instability-admitting Hamiltonian has a much richer spectrum than a stable Hamiltonian, and quantum instability is associated with an almost infinite recurrence time.

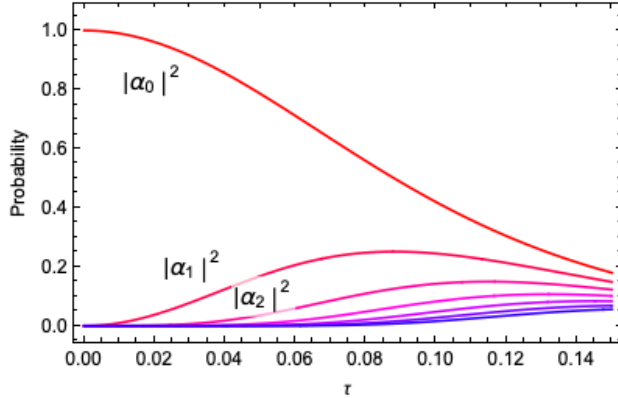


Figure 2: Evolution of the probability of occupation number states for unstable initial condition $(n_{1i}, n_{2i}, n_{3i}) = (100, 0, 0)$ and spreading parameter $\varepsilon = 0$. This corresponds to $\alpha_0 = 1$ and $\Psi = \psi_0$ at $\tau = 0$. The first three states' probabilities are labeled, and the first seven states are plotted.

A. Quantum instability as a wave function cascade in the space of occupation number states

The exponential growth in the occupation numbers shown in Eq. (51) and Fig. 1 is realized through a cascade of wave functions from states with higher $|n_1\rangle$ to states with lower $|n_1\rangle$. This cascade is particularly evident with an initial state which is maximally localized and also maximal in the expectation value of \hat{n}_1 . Show in Fig. 2 is such a probability cascade with initial condition $(n_{1i}, n_{2i}, n_{3i}) = (100, 0, 0)$, which initializes the $\psi_0 = |100, 0, 0\rangle$ state with a probability 1, i.e., $\alpha_0 = 1$ at $\tau = 0$.

Only the first seven states' probability evolution is shown in Fig. 2, but the cascade occurs through all 101 available states as shown in Fig. 3(a). The cascading behavior is characteristic of the instability in the three-wave interaction. In a stable system, with an otherwise identical initial probability distribution among its 101 states, the cascade does not occur as illustrated in Fig. 3(b) for the case of $(n_{1i}, n_{2i}, n_{3i}) = (100, 900, 0)$. It is interesting to note that the cascading process evident in Fig. 3(a) is maintained well past the time when the numerical solution and the approximate linear solution diverge. Also of note in Figs. 3(a) and 3(b) is the irreversibility of the unstable quantum system versus the guaranteed reversibility of the stable quantum system. The recurrence time shown in Fig. 3(b) is approximately 0.1.

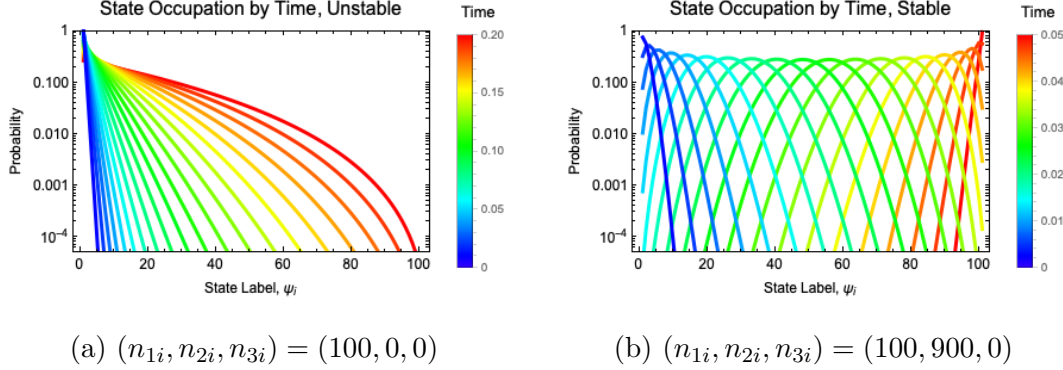


Figure 3: Probability distribution over occupation number states at various times, represented by different colors, for initial condition $\alpha_0^2(0) = 1$. For the unstable case (a), $s_2 = s_3 = 100$, while for the stable case (b), $s_2 = 100$ and $s_3 = 1000$. The unstable initial condition results in a cascade of probability among all 101 states, and the variance monotonically increases. For the stable case, the variance oscillates with a recurrence time of approximately 0.1. Only the first half of the recurrence time is plotted in (b) for clarity.

The unshown second half would overlap with the first half.

B. Spectrum property of quantum instability

In this subsection, we will look closely at the eigenvectors and eigenvalues of the two $d = 101$ systems shown in Fig. 3, with $(s_2, s_3) = (100, 100)$ and $(s_2, s_3) = (100, 1000)$, respectively. The first system admits quantum instability and the second does not. According to the theoretical analysis developed in Sec. III, this is because for the second system, $\gamma_Q^2/4 = \langle n_1 \rangle - \langle n_2 \rangle - \langle n_3 \rangle - 1/2 = 3\langle n_1 \rangle - s_3 - s_2 - 1/2 = 3\langle n_1 \rangle - 999.5 < 0$, since $\langle n_1 \rangle = s_2 - \langle n_3 \rangle < s_2$. The 101 eigenvalues of the two systems are shown in Fig. 4. For the stable system, the eigenvalues are linearly distributed to a high precision, i.e.,

$$\lambda_0 = 0, \lambda_1 \approx 630, \lambda_2 = -\lambda_1, \lambda_3 \approx 2\lambda_1, \dots, \lambda_{100} = -50\lambda_1, \quad (53)$$

while it can be seen in Fig. 4 that the eigenvalues in the unstable case are nonlinearly distributed. For intermediate values of $s_3 > s_2$ and $s_3 < 1000$, it was found that the eigenvalues lie between these two extremes.

The linearity of the eigenvalues of for the stable case places strong limitations on the allowable dynamics of the system. To see this directly, we analyze the frequency decomposition of the expectation of the occupation numbers. Denote by \mathbf{v}_j the eigenvectors of H .

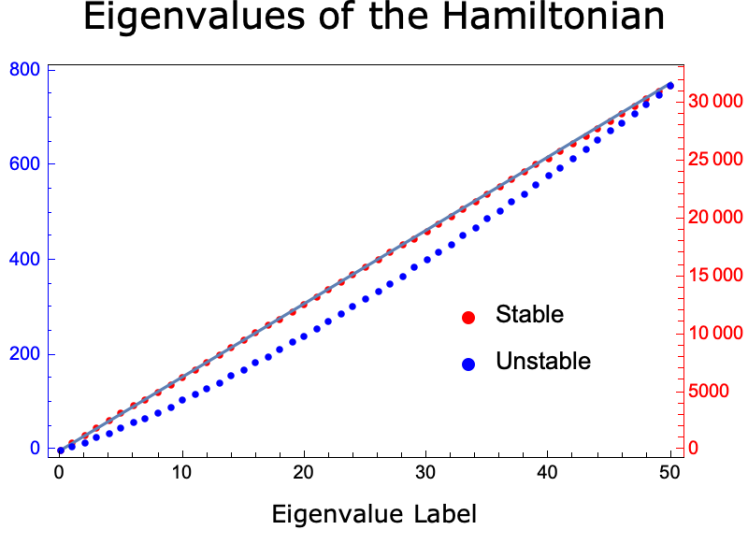


Figure 4: Eigenfrequencies of quantum systems with (red, upper) and without (blue, lower) quantum instability. The unstable system has $s_2 = s_3 = 100$, while the stable system has $s_2 = 100$ and $s_3 = 1000$. Only 51 of the 101 eigenvalues are shown, since the spectra are symmetric with respect to the real axis.

In the ψ_j bases,

$$\mathbf{v}_j = \sum_{k=0}^{s_2} \beta_{jk} \psi_k, \quad (54)$$

which defines the transformation matrix β_{jk} . For a state $\Psi(t)$, we have

$$\Psi(t) = \sum_{j=0}^{s_2} \alpha_j(t) \psi_j = \sum_{j=0}^{s_2} \epsilon_j \mathbf{v}_j e^{-i\lambda_j t}. \quad (55)$$

This then identifies

$$\alpha_j(t) = \sum_{k=0}^{s_2} \epsilon_k \beta_{kj} e^{-i\lambda_k t}, \quad (56)$$

The expectation $\langle n_3 \rangle(t)$ can be evaluated as

$$\langle n_3 \rangle = \sum_{j=0}^{s_2} |\alpha_j(t)|^2 j \quad (57)$$

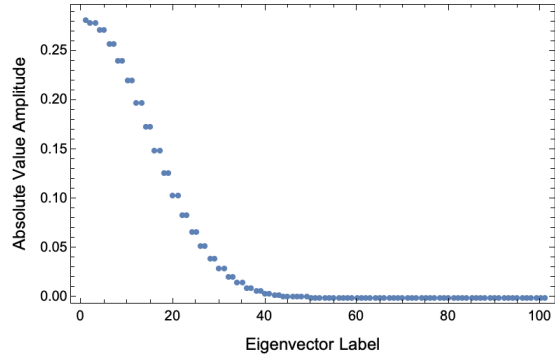
$$= \sum_{j=0}^{s_2} \left| \sum_{k=0}^{s_2} \epsilon_k \beta_{kj} e^{-i\lambda_k t} \right|^2 j \quad (58)$$

$$\begin{aligned} &= \sum_{j=0}^{s_2} \sum_{k=0}^{s_2} |\epsilon_k \beta_{kj}|^2 j \\ &\quad + \sum_{j=0}^{s_2} \left\{ \sum_{k=1}^{s_2} \left[\epsilon_0 \epsilon_k \beta_{0j}^\dagger \beta_{kj} e^{i(\lambda_0 - \lambda_k)t} + c.c. \right] \right. \\ &\quad \quad + \sum_{k=2}^{s_2} \left[\epsilon_1 \epsilon_k \beta_{1j}^\dagger \beta_{kj} e^{i(\lambda_1 - \lambda_k)t} + c.c. \right] + \\ &\quad \quad + \dots \\ &\quad \quad \left. + \epsilon_{s_2-1} \epsilon_{s_2} \beta_{s_2-1,j}^\dagger \beta_{s_2j} e^{i(\lambda_{s_2-1} - \lambda_{s_2})t} + c.c. \right\}. \quad (59) \end{aligned}$$

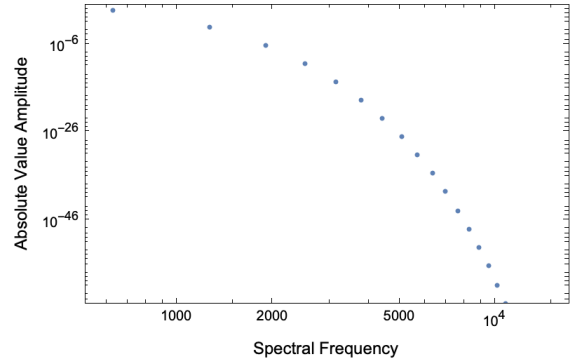
The spectral frequencies available for $\langle n_3 \rangle(t)$ are the differences between each pair of the eigenfrequencies $\lambda_i - \lambda_j$ where $i \neq j$. The weights are determined by the weighting of eigenvectors, ϵ_i , and the transformation matrix β_{kj} .

For the stable quantum Hamiltonian with $(s_2, s_3) = (100, 1000)$ defined above, the linear spacing of its eigenvalues means that there are only 101 spectral frequencies (corresponding to combinations of the 50 distinct eigenvalue absolute values and the 0 eigenvalue) available for $\langle n_3 \rangle(t)$. It also implies that its spectrum constitutes a Fourier series. By contrast, the unstable Hamiltonian with $(s_2, s_3) = (100, 100)$ has $\text{Floor}(d^2/4) + 1 = 2551$ spectral frequencies available. The values of the spectral frequencies, not just their quantity, are also important. The maximum recurrence time, when the system will begin to repeat itself, in either system will be the least common multiple of the spectral periods. For the stable Hamiltonian, this value is guaranteed to exist, since the Fourier periods will all be rational multiples of a single, base period. Conversely, we expect an exact recurrence time to never exist in the unstable system. Exact analytical solutions to the eigenvalues of even low-dimensional Hamiltonians show that the spectral frequencies are incompatibly irrational, implying an almost infinite recurrence time. This irreversibility is a familiar hallmark of instability in a classical system.

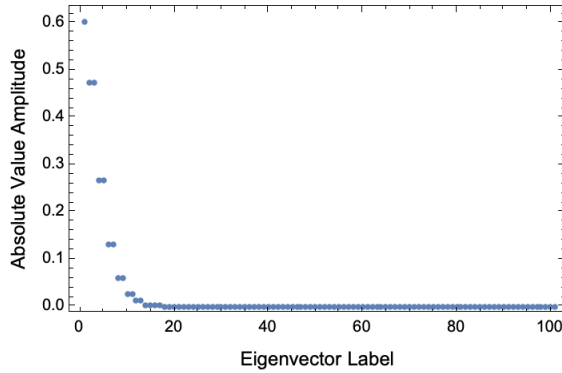
The amplitude of eigenvalues and frequency spectrum of the stable and unstable systems given the initial condition $\alpha_0(0) = 1$ are plotted in Fig. 5. The unstable system is $(s_2, s_3) =$



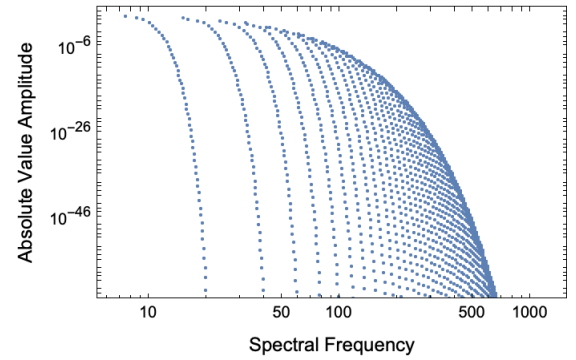
(a) Amplitude of eigenvectors, ϵ_i , for the stable system.



(b) Spectrum weight of $\langle n_3 \rangle(t)$ for the stable system.



(c) Amplitude of eigenvectors, ϵ_i , of the unstable system.



(d) Spectrum weight of $\langle n_3 \rangle(t)$ for the unstable system.

Figure 5: Eigenvector weights ϵ_i and spectrum weight of $\langle n_3 \rangle(t)$ (the coefficients $\epsilon_i \epsilon_j \beta_{ik} \beta_{jk}$ for each frequency $\lambda_i - \lambda_j$ in Eq. (59)) for the stable $(s_2, s_3) = (100, 1000)$ and unstable $(s_2, s_3) = (100, 100)$ systems. The initial condition is $\alpha_0 = 1$, which corresponds to the $\psi_0 = |100, 0, 0\rangle$ mode having probability 1. Most of the 101 and 2551 spectral modes have zero amplitude in (b) and (d), respectively, and are not displayed.

$(100, 100)$ with $(n_{1i}, n_{2i}, n_{3i}) = (100, 0, 0)$, and the stable system is $(s_2, s_3) = (100, 1000)$ with $(n_{1i}, n_{2i}, n_{3i}) = (100, 900, 0)$. The spectral differences between the stable and unstable quantum systems discussed above are evident.

V. DISCUSSION AND CONCLUSIONS

For a static, finite-dimensional Hermitian quantum system, all eigenfrequencies of the system are real, and the dynamics is unitary. However, this does not preclude exponential growth of the expectations of observables that do not commute with the Hamiltonian. In the present study, quantum instability is defined as a solution for which the expectation of an observable deviates exponentially relative to an initial value. The quantum theory of the three-wave interaction, obtained by quantizing the classical Hamiltonian using a field-theoretical method, maps the nonlinear classical Hamiltonian into a finite-dimensional Hermitian system. We have shown that the quantum theory admits a quantum instability corresponding to the classical three-wave instability. The quantum and classical descriptions of the three-wave instability require the same conditions to occur, with the quantum theory having additional requirements on the variance of its initial condition. In the classical limit, both theories predict the same growth rate. We numerically demonstrated that this quantum instability is realized as a cascade of wave functions in the space of occupation number states, and further showed that such a cascade does not occur with a stable Hamiltonian. It is possible that other instabilities described by classical theory, especially the opto-mechanical instability [1-3], are also realized quantum mechanically through a cascade of wave functions in the space of occupation number states. The Hamiltonian of an unstable quantum system is shown to possess a much richer spectrum than the Hamiltonian of a stable quantum system. Additionally, the unstable quantum system exhibits irreversibility, while the stable system has a relatively small recurrence time.

Future work would aim to characterize other quantum instabilities and develop a general framework for their recognition and correspondence with classical systems. It is possible that the three-wave interaction and other physical processes may admit quantum instabilities which have no classically unstable counterparts. Finding these native quantum instabilities would provide stronger motivation for the definition of quantum instability proposed in the present study.

Current technology allows for the quantum three-wave instability to be simulated using a quantum hardware. The work performed by Shi *et al.* in simulating the quantum three-wave interaction utilized only two qubits and three of their four possible states, $|00\rangle$, $|01\rangle$, and $|10\rangle$, to represent $d = s_2 + 1 = 3$ states [14]. Although the linear solution given by Eq. (51)

could have been simulated, the growth rate of the quantum instability would have been too small to notice at such a low dimension. Also, the dimension was too small to compare with the classical instability. However, since the number of states representable by n qubits is $d \propto 2^n$, quantum hardware with sufficient numbers of qubits to simulate the quantum instability and compare to the classical instability already exist [32]. Of course, this issue is complicated by the unitary operator needing $d^2 = 2^{n^2}$ gates to be approximated using the gates available to the system. Though the method of implementing a single, special-made gate as in [14] somewhat mitigates this problem.

ACKNOWLEDGMENTS

This research was supported by the U.S. Department of Energy (DE-AC02-09CH11466).

-
- [1] M. Ludwig, B. Kubala, and F. Marquardt, *New J. Phys.* **10**, 095013 (2008).
 - [2] S. Bennett and A. Clerk, *Phys. Rev. B* **74**, 201301 (2006).
 - [3] D. Rodriguez, J. Imbers, T. Harvey, and A. Armour, *New J. Phys.* **9**, 10.1088/1367-2630/9/4/084 (2007).
 - [4] G. Casati, B. Chirikov, F. Izraelev, and J. Ford, *Lecture notes in physics* (Springer, Berlin, Heidelberg, 1979) Chap. Stochastic behavior of a quantum pendulum under a periodic perturbation.
 - [5] J. Bellissard, *Schrödinger operators* (Springer, 1985) Chap. Stability and instability in quantum mechanics, pp. 204–229.
 - [6] C. M. Bender and S. Boettcher, *Physical Review Letters* **80**, 5243 (1998).
 - [7] C. M. Bender, D. C. Brody, and H. F. Jones, *Physical Review Letters* **89**, 270401 (2002).
 - [8] C. M. Bender, *Reports on Progress in Physics* **70**, 947 (2007).
 - [9] A. Mostafazadeh, *Journal of Mathematical Physics* **43**, 205 (2002).
 - [10] H. Qin, R. Zhang, A. S. Glasser, and J. Xiao, *Physics of Plasmas* **26**, 032102 (2019).
 - [11] H. Qin, Y. Fu, A. S. Glasser, and A. Yahalom, *Physical Review E* **104**, 015215 (2021).
 - [12] R. Zhang, H. Qin, and J. Xiao, *Journal of Mathematical Physics* **61**, 012101 (2020).
 - [13] I. Dodin and E. Startsev, *Phys. of Plasmas* **28**, 092101 (2021).

- [14] Y. Shi, A. Castelli, J. Wu, V. Geyko, F. Graziani, S. Libby, J. Parker, Y. Rosen, L. Martinez, and J. DuBois, *Phys. Rev. A* **103**, 062608 (2021).
- [15] J. Moody, P. Michel, L. Divol, R. Berger, E. Bond, D. Bradley, D. Callahan, E. Dewald, S. Dixit, M. Edwards, and et al., *Nat. Phys.* **8**, 10.1038/nphys2239 (2012).
- [16] J. Myatt, J. Zhang, R. Short, A. Maximov, W. Seka, D. Froula, D. Edgell, and et al., *Phys. Plasmas* **21**, 055501 (2014).
- [17] V. Zakharov, V. L'vov, and G. Falkovich, *Kolmogorov Spectra of Turbulence I: Wave Turbulence* (Springer, New York, 2012).
- [18] L. Frantz and J. Nodvik, *J. Appl. Phys.* **34**, 10.1063/1.1702744 (1963).
- [19] J. Ahn, A. Efimov, R. Averitt, and A. Taylor, *Opt. Express* **11**, 10.1364/OE.11.002486 (2003).
- [20] G. Brunton, G. Erbert, D. Browning, and E. Tse, *Fusion Eng. Des.* **87**, 10.1016/j.fusengdes.2012.09.019 (2012).
- [21] Y. Shi, *Plasma Physics in Strong Field Regimes*, Ph.D. thesis, Princeton University (2018).
- [22] M. Rosenbluth, R. White, and C. Liu, *Phys. Rev. Lett.* **31**, 1190 (1973).
- [23] V. Zakharov and S. Manakov, *Sov. Phys. JETP* **42** (1976).
- [24] D. J. Kaup, A. Reiman, and A. Bers, *Reviews of Modern Physics* **51**, 275 (1979).
- [25] A. Reiman, *Reviews of Modern Physics* **51**, 311 (1979).
- [26] K. Ohkuma and M. Wadati, *J. Phys. Soc. Jpn.* **53**, 2899 (1984).
- [27] Y. Shi, H. Qin, and N. J. Fisch, *Physical Review E* **96**, 023204 (2017).
- [28] Y. Shi, H. Qin, and N. J. Fisch, *Physics of Plasmas* **28**, 042104 (2021).
- [29] R. Sagdeev and A. Galeev, *Nonlinear Plasma Theory* (W. A. Benjamin, Inc., New York, 1969).
- [30] A. Jurkus and P. N. Robson, *Saturation effects in a travelling-wave parametric amplifier*, Vol. 107 (Proceedings of the IEE-Part B: Electronic and Communication Engineering, 1960).
- [31] E. T. Jaynes and F. W. Cummings, *Comparison of quantum and semiclassical radiation theories with application to the beam maser*, Vol. 51 (Proceedings of the IEEE, 1963).
- [32] <https://www.rigetti.com/what-we-build> (2021).